SSRG International Journal of Civil Engineering
ISSN: 2348-8352/https://doi.org/10.14445/23488352/IJCE-V10I6P109

Volume 10 Issue 6, 86-94, June 2023

Original Article

Stability Analysis of High Slopes in Mines Based on Slide and Midas

WANG Maoxuan[1], LI Hanlin[2], JIN Xiaoguang[3]

[1,2,3]*Chongqing University, China*

[1]*Corresponding Author: wmxcqu@qq.com*

Received: 01 April 2023 Revised: 28 May 2023 Accepted: 15 June 2023 Published: 30 June 2023

Abstract *- Stable high slopes in mines are a prerequisite for sustained and efficient mining operations. In order to analyze the stability of slopes under different working conditions, a high slope in a mine in Chongqing was taken as the research object. The limit equilibrium method in Slide software was used to conduct slope stability analysis for the mine slope under three different conditions: natural, blast force, and seismic force. The corresponding slope stability coefficients were obtained. Then, the stability analysis of the slope under three conditions: natural, rainfall, and seismic force, was carried out using the strength reduction method in Midas software. The results showed that the slope was stable under all the analyzed conditions. However, due to the different analysis principles, parameter types, and boundary conditions used in the two methods, there were differences in the calculation results of the safety factors. Finally, based on the numerical simulation results, the weak points and their variation patterns of the slope under different working conditions were identified, providing valuable insights for the stability analysis of similar slopes.*

Keywords *- Numerical simulation, Rocky slope, Rainfall seepage, Seismic force, Stability analysis.*

1. Introduction

Mining operations are crucial for energy extraction in China, and during the construction process, slope instability may occur in mining areas [1]. The safety and stability of mining slopes directly affect product safety, especially for high slopes in complex geological conditions, which have been the focus of stability analysis research. In recent years, computers have been widely applied in evaluating stability and analysis of failure modes in rock slopes, with numerical simulation methods demonstrating significant advantages over traditional analysis methods [2].

Currently, the limit equilibrium method is the most widely used slope stability analysis method in domestic and international applications, representing traditional slope stability analysis methods [3]. Asfaw Legesse et al. [4] employed the limit equilibrium method to analyze the stability of embankment shoulder slopes and identified potentially unstable slopes under saturated conditions. The finite element strength reduction method is a typical numerical analysis method and is presently one of the most widely used numerical analysis methods. Sarkar Sourav et al. [5] studied the stability of double-layer slopes using the strength reduction method.

They proposed feasible measures to improve slope stability under specific conditions, confirming the applicability of this method for analyzing slope stability. This study selected a high slope in a specific mine as an example. The slope is located in the northern segment of the syncline axis, which extends in the N20°E direction within the mining area. The ore layers exhibit a banded distribution in the mining area, with dip directions of 280° to 315° and dip angles ranging from 18° to 53° in the northwest wing, and dip directions of 95° to 114° and dip angles ranging from 11° to 33° in the southeast wing. The mining area's exposed formations and surroundings mainly consist of Quaternary strata (Q_4) and Triassic Lower Jialingjiang Formation (T_1j) strata. The primary mining target is the third segment (T_1j^3) of the Triassic Lower Jialingjiang Formation, with a thickness of 180-210 meters.

Based on the engineering geological survey data, the Slide (Limit Equilibrium Method) and Midas (Strength Reduction Method) was employed to analyze the stability of the high slope under three different working conditions, obtaining the corresponding safety factors. Deformation and failure development trends of the slope under various conditions were analyzed based on the calculation results,

and effective suggestions were proposed from the perspective of finite element analysis.

2. Rock Mechanics Parameters and Working Load Parameters

2.1. Determination of Rock Mechanics Parameters

The rock mechanics parameters of the high slope in this mine were determined based on the mining rock and soil physical mechanics test report, the "Technical Specifications for Open-pit Mine Slope Engineering" (GB51016-2014) (Table 1), and relevant research literature. These parameters are listed in Table 2.

2.2. Load Parameter Values

2.2.1. Seismic Force Parameters Values

According to the "China Seismic Ground Motion Parameter Zonation Map" (GB18306-2015) and the "Code for Seismic Design of Buildings" (GB50011-2010 (2016 edition)), the peak ground acceleration for seismic motion in this area is 0.05g, the characteristic period of the seismic response spectrum is 0.35s. The seismic intensity is classified as level VI. There have been no reports of solid earthquake activity in this area or its neighbouring regions in recent years, indicating that the mining area is in a low-seismicity zone with good regional stability.

2.2.2. Rainfall Parameter Values

According to relevant meteorological data, the mining area lies within the subtropical monsoon climate zone of the Sichuan Basin. The region experienced abundant rainfall, with the maximum daily rainfall recorded as 141.4mm on May 24, 1964. When simulating working conditions under rainfall, the mechanical properties of the rock mass in a saturated state, known as the saturated strength, are used as the basis for calculations.

2.2.3. Slope Safety Factor Values

According to the "Technical Specifications for Open-pit Mine Slope Engineering" (GB51016-2014), the safety factor is an essential parameter for assessing slope stability and serves as a crucial threshold. The stability factor is calculated by comparing the comprehensive resistance force to sliding with the comprehensive driving force on the potential sliding surface. A stability factor greater than or equal to 1 indicates a stable state, while a value less than 1 indicates an unstable state.

Based on the "Technical Specifications for Open-pit Mine Slope Engineering" (GB51016-2014), the overall safety level of the slope in this mine is classified as level II. The values of the slope safety factor under three different working conditions can be found in Table 3.

3. Limit Equilibrium Method Stability Analysis

3.1. The Solution Principle of Slide Stability Analysis

The limit equilibrium method is a traditional approach to slope stability analysis. It evaluates the stability of a slope quantitatively using safety factors. Due to the visual nature of safety factors, it is widely applied in engineering. This method is based on the theory of rigid-plastic mechanics, focusing only on the deformation mechanism at the moment of soil failure and disregarding the soil deformation process. It only requires the balance of forces and moments and follows the Mohr-Coulomb criterion.

The basic idea of this method is to assume a potential sliding surface based on experience and theories. The stability of the slope under its load can be calculated by analyzing the balance between the external forces acting on the soil and the resistance provided by its internal strength near the point of failure. The limit equilibrium method does not solve the fundamentally indeterminate problem by introducing stress-strain relationships as in traditional elastoplastic mechanics. Instead, it directly assumes certain surplus unknowns to achieve an equal number of equations and unknowns, making the problem statically determinate and solvable.

Based on the boundary conditions of slope failure and the application of mechanics analysis, theoretical calculations and mechanical analysis of the anti-sliding strength were carried out for potential sliding surfaces under various load conditions. By repeated calculations and comparative analysis, stability factors were determined for the potential sliding surfaces.

3.2. Selection of Slope Profiles

Based on the reserve report of the Jucheng Mine in Chongqing for the first half of 2022 for building stone materials using limestone, the most unfavourable 2-2' was selected as the analysis profile (Figure 1). Based on this, a slope analysis model was established, as shown in Figure 2.

3.3. Slope Calculation Results

Based on calculations, the stability factor results for the 2-2' profile under three different load combinations, namely Load Combination I, Load Combination II, and Load Combination III, are shown in Table 4. The calculation results show that the safety factors obtained using the Bishop and Janbu methods differ for the three load combinations. The stability factor calculated using the more conservative Janbu method was selected as the minimum safety factor. Analysis of the calculation results in Table 4 indicates that the overall slope stability of the mine's slope profile satisfies the relevant specifications and requirements.

The slope parameters selected for the design are reasonable and reliable [5]. During the subsequent mining process, it is crucial to consider the influence of rainfall on slope stability and strengthen the prevention and control measures against blasting impacts. Although the stability factors of the slope under the three load combinations meet the requirements for safe slope stability, continuous external factors such as rainfall, blasting, and seismic activities can reduce slope stability and increase the probability of slope instability occurrences.

4. Strength Reduction Method Stability Analysis

Based on the Slide limit equilibrium method research, the stability of the slope profile 2-2' under natural (self-weight + groundwater), natural + rainfall, and natural + seismic conditions were analyzed using the GTS-NX (Strength Reduction Method) numerical simulation technique.

4.1. Basic Principles and Criteria of MIDAS GTS NX

The calculation process for slope stability in MIDAS/GTS NX adopts the Strength Reduction Method. The principle of the Strength Reduction Method is to reduce the strength parameters of the soil and rock mass in the ideal elastoplastic constitutive model. By continuously reducing these parameters, different values of the strength reduction coefficient (c and φ) are obtained until the soil and rock mass reaches failure. The resulting reduction coefficient represents the stability factor. The reduction of the strength parameters is performed according to Equations 1 and 2.

$$c_f = c/F \tag{1}$$

$$\varphi_f = arctan\left(\frac{tan\varphi}{F}\right) \tag{2}$$

In the equations, c and φ represent the cohesion and internal friction angle of the rock or soil mass, c_f and φ_f represent the reduced cohesion and internal friction angle of the rock or soil mass, and F is the reduction coefficient. The stability factor is calculated, and the non-convergence of the calculation for all elements is used as the criterion for slope stability evaluation.

4.2. Establishment of Numerical Analysis Model

The mine's slope profile 2-2' was selected for stability numerical simulation analysis. The slope model is divided into four soil and rock layer types based on the geological survey report and the actual soil layer distribution. The upper four layers consist of alternating distribution of dolomite and karstic breccia, and the lower three layers consist of limestone layers with an interlayer of weakly cemented marl. The profile was imported into the Midas software, and during the mesh division, the element type was set as triangles + quadrilaterals.

The mesh was denser at the slope surface landslide body location with a mesh size of 2m, while it was slightly sparser at other boundary locations with a mesh size of 2.5m. After the model was established, the overall slope height was 142m, the length was 195m, the total number of nodes was 3941, and the total number of elements was 3830. In order to represent the actual situation of the mine slope more realistically, it is necessary to consider the distribution of initial pore water pressure in the slope. In the Midas seepage/consolidation module, the model's left and right water head boundaries were set based on the water level at the left and right boundaries. The numerical calculation model established is shown in Figure 3.

4.3. Slope Calculation Results

4.3.1. Stability Analysis of the Slope in Natural Condition

The selected calculation method is the Strength Reduction Method, which has been verified for its application in searching the plastic zone of rock slopes by Shiferaw Henok Marie [6] and S. M. Seyed-Kolbadi [7]. Analyze the deformation and stress conditions of a simulated slope under self-weight conditions, considering the presence of groundwater, and obtain the displacement-strain contour map in its natural state. Through simulation calculations, the stability factor of the slope under natural conditions was determined to be 2.100. The displacement cloud maps in the horizontal and vertical directions of the slope are shown in Figure 4.

The maximum horizontal displacement is 5.5 cm, located at the bottom of the slope in the marl layer. Monitoring of the deformation in the marl layer should be emphasized, and feedback information should be provided promptly. The maximum vertical displacement is 9.6 cm, located at the interface between the uppermost karstic breccia and dolomite layers at the top of the slope. The practical plastic strain cloud map is shown in Figure 5. The distribution of effective plastic strain in the slope is concentrated in the weak interlayer and at the slope toe, with more significant values observed at the slope angles. Regular inspections should be conducted to monitor the deformation of the slope toe.

4.3.2. Slope Stability Analysis under Rainfall Condition

Rainfall is a common factor that can cause slope deformation and failure [8]. This section considers the influence of rainfall conditions on the stability of high mining slopes. The same numerical simulation model as in the previous section was used to facilitate a comparative

analysis of the slope stability under self-weight conditions. The mesh division and physical parameters remained consistent to avoid errors caused by differences in element division. Since the slope is composed of rock, the unsaturated characteristics of rainfall infiltration have minimal impact compared to soils.

Therefore, the saturated unit weight of various rocks was used in the simulation calculations. The initial water level remained the same as under natural conditions, considering only the stability of the slope under rainfall conditions. Based on local meteorological data, the worst-case scenario with a maximum daily rainfall of 141.4 mm was selected for analysis over two consecutive days. The stability factor of the slope under rainfall conditions was determined to be 1.775. The displacement cloud maps in the horizontal and vertical directions of the slope under rainfall conditions are shown in Figure 6.

The maximum horizontal displacement, previously located at the bottom of the weak interlayer (marl), was now widely distributed in the lower portion of the arc-shaped landslide mass, with a maximum horizontal displacement of 5.0 cm at the bottom of the landslide's toe. Compared to the deformation characteristics under natural conditions, the vertical displacement in the slope below the weak rock layer significantly increased, with a maximum vertical displacement of 7.9 cm and evident compression deformation at the toe of the slope. The displacement changes occur due to increased rainfall intensity and infiltration velocity under rainfall conditions. When rainwater infiltrated the weak interlayer, the poor permeability of the marl layer affected the flow path, resulting in significant changes in the displacement of the slope below the weak interlayer and forming an arc-shaped landslide mass.

The practical plastic strain cloud map of the slope under rainfall conditions is shown in Figure 7. It can be observed that the values of effective plastic strain increased, and the range of the plastic zone underwent specific changes under rainfall conditions. Compared to the natural state, the effective plastic strain at the weak interlayer disappeared, and the effective plastic strain concentrated at the toe of the slope.

4.3.3. Slope Stability Analysis under Seismic Condition

Under seismic conditions, slopes are subjected to dynamic loads. Under dynamic loads, the soil in the slope experiences inertial forces and cyclic degradation, leading to a further decrease in shear strength and an increase in the sliding force in the slope. Eventually, the slope's original stability is compromised, resulting in a decreased safety factor and potential slope instability [9]. To facilitate a comparative analysis of the slope's stability under natural conditions, the calculation model still adopted the model for the natural condition. Based on this, this study used the horizontal component of the El-Centro seismic wave as the load acting on the slope under seismic conditions.

The seismic intensity in the region where the slope is located was determined to be level VI, with a peak ground acceleration of 0.05g. Therefore, the seismic wave needed to be scaled down. Given that the peak acceleration of the seismic wave is 0.3569g (at time=2.14s), a scaling coefficient of 0.14 was set. The linear time history analysis and equivalent nodal force analysis method in Midas-GTS were used. First, the grid point forces were selected in the output control during the linear time history analysis. Since the seismic wave reaches its peak acceleration at 2.14s, the maximum displacement of the slope occurs near this moment. Therefore, the forces acting on the slope now needed to be analyzed. The equivalent nodal forces corresponding to 2.14s were extracted from the linear time history analysis results, and these forces were applied to the slope model for the SRM stability analysis.

The stability factor of the slope under seismic conditions was determined to be 1.506. The displacement cloud maps in the horizontal and vertical directions of the slope are shown in Figure 8. The maximum horizontal displacement was concentrated near the weak interlayer and is more pronounced than the natural state, with a maximum displacement value of 11.8 cm. The maximum vertical displacement is similar to the natural condition and occurs at the top of the slope, but it is noticeably more extensive, with a maximum value of 18.2 cm. Figure 8 shows that the seismic action affects the distribution of displacements in the horizontal direction of the slope.

This is because the shear resistance of the weak interlayer is much lower than that of other rock layers. The seismic action had a more significant influence on the horizontal forces, and there were discontinuity surfaces between the mudstone and limestone layers, leading to relative inhomogeneity within the rock layers. When the seismic wave propagated through the layers, the rock and soil particles in the layers underwent horizontal vibration, generating inertial forces (F=ma). These inertial forces created additional stresses in the slope, resulting in shear and tensile stresses between the discontinuity surfaces that are greater than the shear strength and tensile strength of the rock layer structure, ultimately causing sliding between the layers.

The slope in question is reverse-layered, and due to the orientation of each rock layer and its self-weight, the slope did not slide downward along the weak interlayer but exhibited significant horizontal displacement on the surface of the weak interlayer. It should be noted that under this level

of seismic motion, the slope does not immediately undergo instability, but repeated seismic loading can lead to internal damage of the rock mass within the slope, eventually resulting in instability. The practical plastic strain cloud map of the slope under seismic conditions is shown in Figure 9. Compared to the practical plastic strain cloud map under natural conditions, the values of effective plastic strain increased, and the location of plastic zones was concentrated on the surface of the weak interlayer without a precise band-like distribution. The reason for the concentration of the damage zone near the weak interlayer under seismic action is that the tensile strength of the rock mass had a significant influence on slope stability.

The mudstone in the weak interlayer had a low tensile strength, and there were tensile and shear stresses between the rock masses under seismic action. When these stresses exceed the shear strength of the rock, the rock mass fails, resulting in significant displacements in practical engineering. Hence, significant displacements and deformations occurred in the slope under seismic action, particularly in the vicinity of the weak interlayer. In summary, the values of maximum horizontal and vertical displacements did not change significantly under rainfall conditions, but the distribution of effective plastic strains underwent noticeable changes. Under seismic conditions, the maximum horizontal and vertical displacements increased, and the concentrated distribution of effective plastic strains shifted from the slope angle to the weak interlayer. The stability factor can be directly read in the post-processing of the calculation results.

Table 1. Recommended values for rock mechanics parameters of the slope

Rock mass basic quality grade	γ(kN/m^3)	Peak shear strength		E (GPa)	μ
		ϕ (°)	c (MPa)		
I	>26.5	>60	>2.1	>33	<0.2
II		60~50	2.1~1.5	33~20	0.2~0.5
III	26.5~24.5	50~39	1.5~0.7	20~6	0.25~0.3
IV	24.5~22.5	39~27	0.7~0.2	6~1.3	0.3~0.35
V	<22.5	<27	<0.2	<1.3	>0.35

Table 2. Selected rock mechanics parameters for the slope

Rock mass	γ(kN/m3)	Compressive strength saturated natural	E(Gpa)	μ	C(Mpa)	ϕ (°)
Dolomitic limestone T_1j^2	27	39-42	2.1	0.33	0.42	34
Limestone T_1J^3	27	47-57	2.2	0.30	0.50	37
Argillaceous limestone T_1J^3	24	/	1.6	0.33	0.35	36
Karstic conglomerate T_1J^2	25	2.1-3.2	1.2	0.40	0.26	26

Table 3. Selection of values for mine slope safety factors

Slope Engineering Safety Grade	Safety Factors for Slope Engineering Design		
	Combination I (self-weight + groundwater)	Combination II (self-weight + groundwater + blast force)	Combination III (self-weight + groundwater + seismic force)
II	1.20	1.18	1.15

Table 4. Stability calculation results for the 2-2' profile under three load combinations

Selected Profile		Minimum Safety Factor	Allowable Safety Factor	Analytical Method
2-2' Profile	Combination I	1.772	1.20	Bishop
		1.670		Janbu
	Combination II	1.702	1.18	Bishop
		1.589		Janbu
	Combination III	1.657	1.15	Bishop
		1.538		Janbu

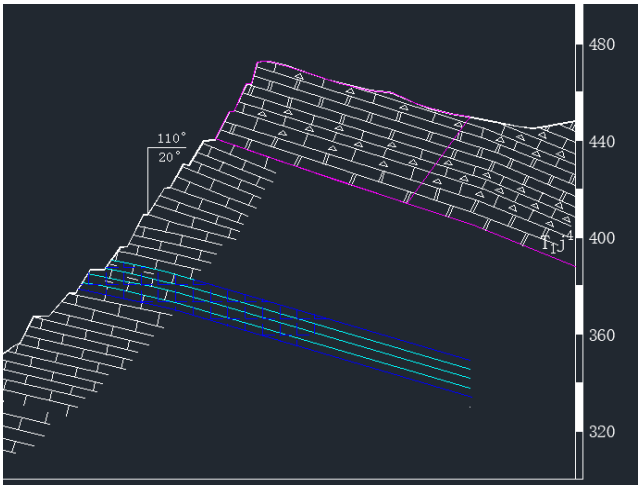

Fig. 1 Schematic diagram of Section 2-2'

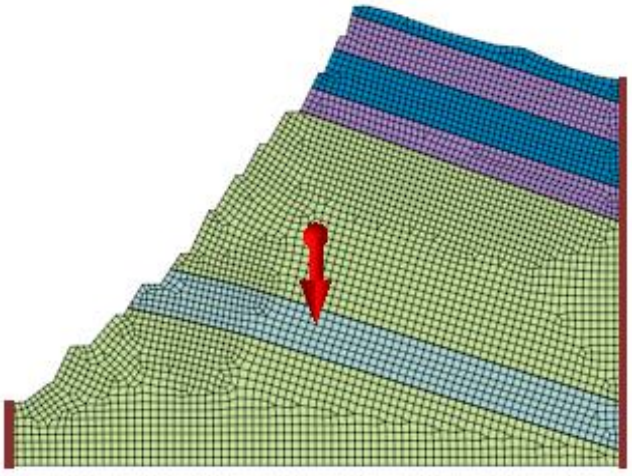

Fig. 3 Numerical model of the cross section 2-2'

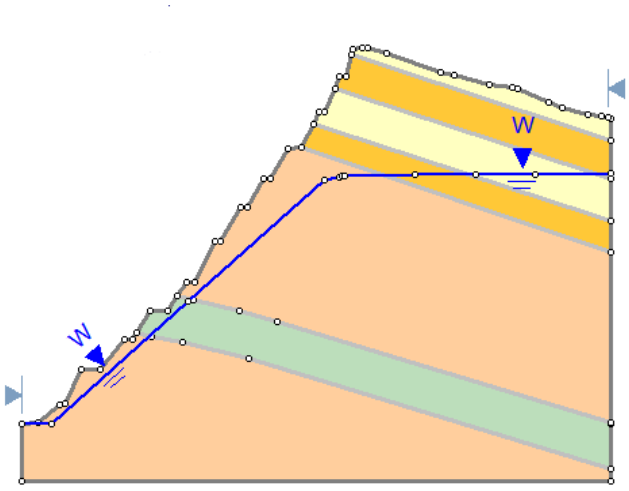

Fig. 2 Slope analysis model

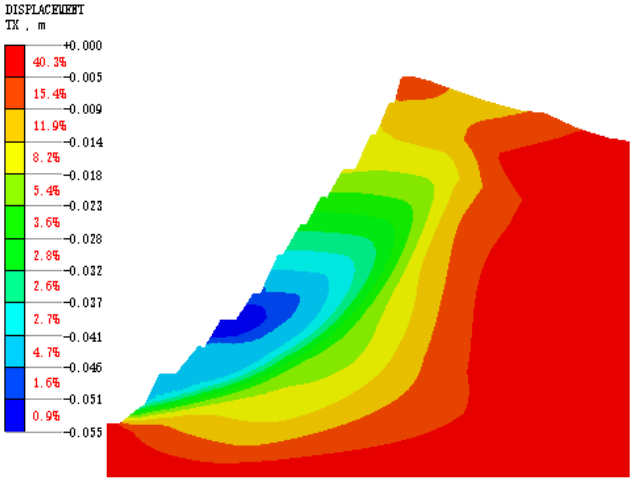

(a) Horizontal displacement

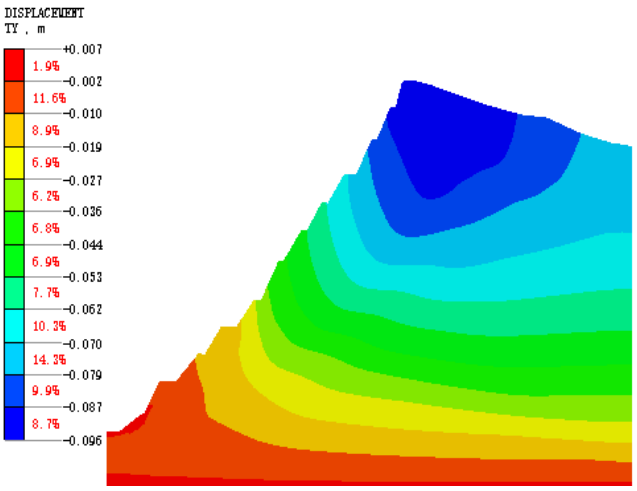

(b) Vertical displacement

Fig. 4 Displacement contour map under natural condition

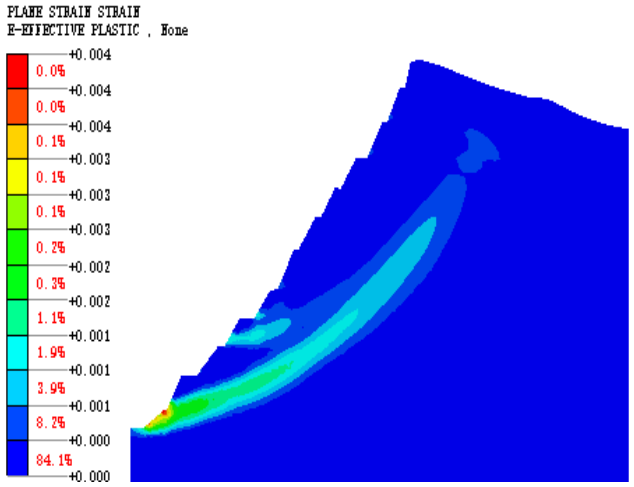

Fig. 5 Contour map of effective plastic strain under natural conditions

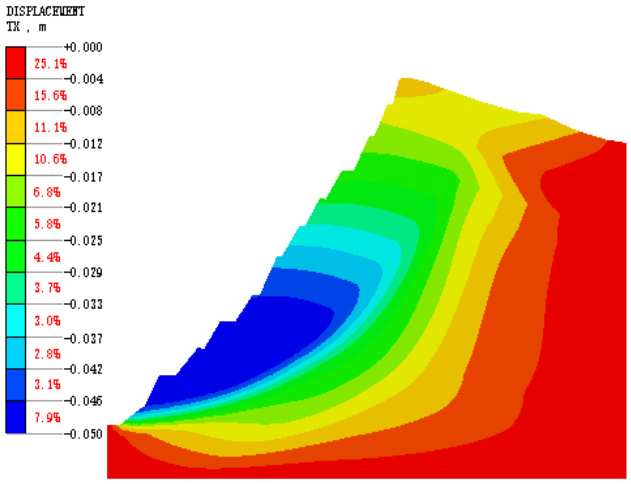

(a) Horizontal displacement

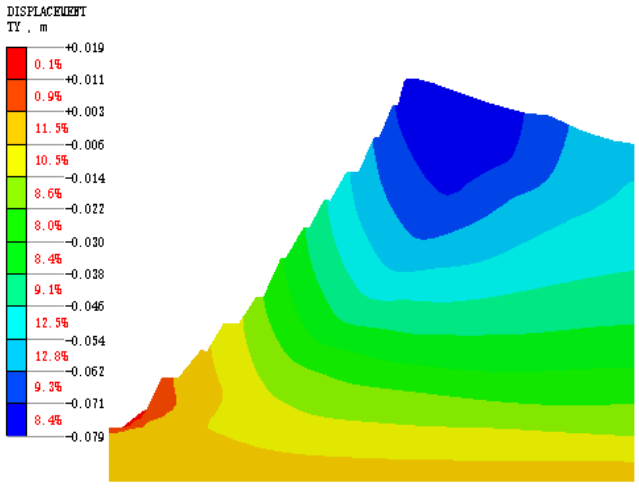

(b) Vertical displacement

Fig. 6 Displacement contour map under rainfall condition

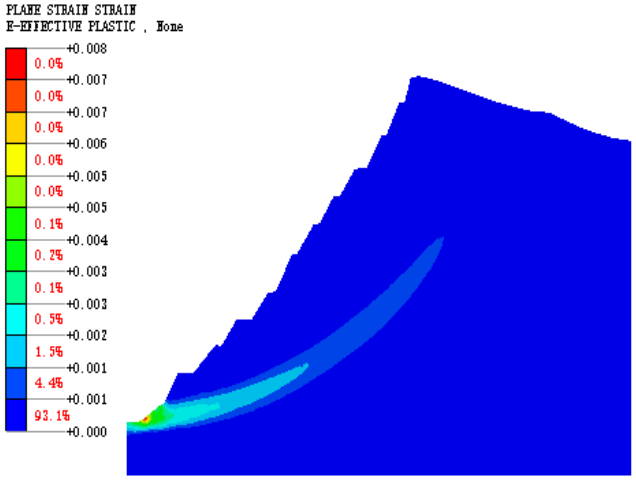

Fig. 7 Contour map of effective plastic strain under rainfall condition

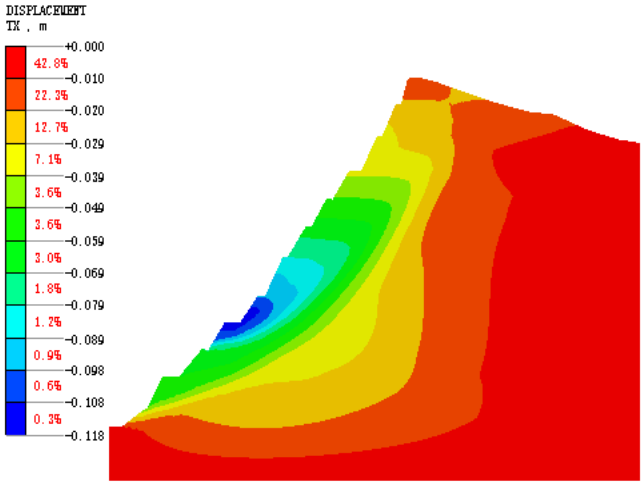

(a) Horizontal displacement

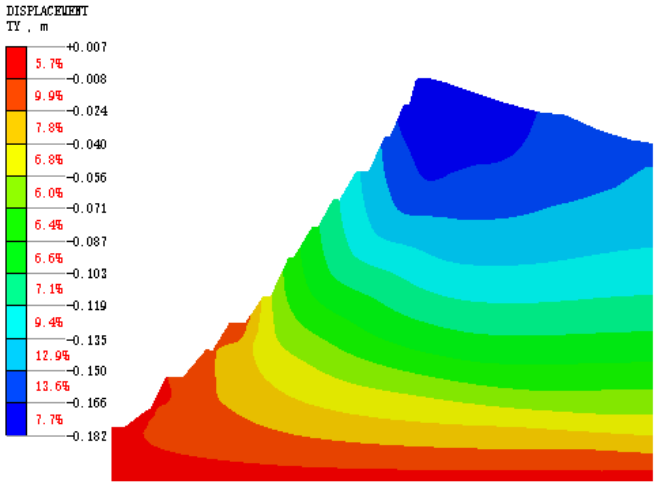

(b) Vertical displacement

Fig. 8 Displacement contour map under the seismic condition

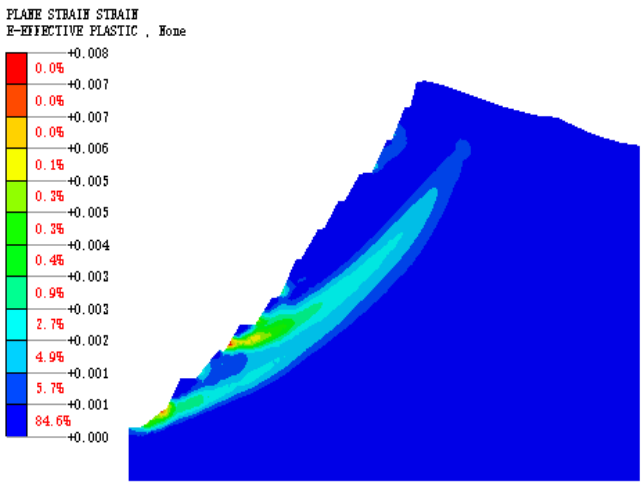

Fig. 9 Contour map of effective plastic strain under the seismic condition

The safety factor decreased in each case, indicating that the slope was relatively more dangerous under rainfall conditions and most dangerous under seismic conditions. The stability factors of the slope under the three conditions were determined to be 2.100, 1.775, and 1.506, respectively. Compared to the Slide results, there were significant differences in the stability factors under natural conditions.

This difference may be because Slide used the coordinates of the original water level to determine the water level. In contrast, Midas determined the water level position by setting water heads at the left and right boundaries. Furthermore, the principles of the two analysis methods were different, leading to variations in the stability factors.

5. Conclusion

This article analyzed the stability of a high slope in the mining area under different working conditions using the limit equilibrium method and the finite element strength reduction method. The conclusions obtained are as follows:

- The limit equilibrium analysis indicates that the minimum safety factors under the three combination conditions of natural force, blasting, and seismic force were 1.772/1.670, 1.702/1.589, and 1.657/1.538, respectively. The Bishop method yielded more conservative results compared to the simplified Bishop method. The slopes under all three combination conditions were stable.
- Numerical simulations using the finite element strength reduction method reveal that the safety factors for the slope in the mining area under natural force, rainfall, and seismic force were 2.100, 1.775, and 1.506, respectively. The slope remained stable under all these conditions, but the safety factors decreased due to rainfall and seismic activity. Additionally, the distribution characteristics of effective plastic strain and maximum displacement of the slope also underwent significant changes.
- There were specific differences in the safety factor values obtained through the limit equilibrium and finite element strength reduction methods. These differences can be attributed to the differences in analysis principles, parameter types, and boundary conditions employed by the two methods.

Funding Statement

This work was supported by the National Key R&D Program of China (2021YFB3901402).

References

[1] Chen Qilin, and Yao Luo, “Stability Analysis and Landslide Early Warning Technology for Steep Slopes in Mines,” *World Nonferrous Metals*, 2021.

[2] Yang Jianhua et al., “Study on Rock Slope Stability Analysis and Support Scheme Based on Midas/GTS Software,” *Electric Survey and Design*, 2022.

[3] Mahyar Arabani, and Hamed Haghsheno, “The Effect of Cohesion Heterogeneity and Anisotropy in c-φ Soils on the Static and Seismic Bearing Capacity of Shallow Foundations,” *Innovative Infrastructure Solutions*, vol. 8, no. 127, 2023. [CrossRef] [Google Scholar] [Publisher link]

[4] Legesse Asfaw, Matebie Meten, and Tola Garo, "Leakage and Abutment Slope Stability Analysis of Arjo Didesa Dam Site, Western Ethiopia," *Arabian Journal of Geosciences*, vol. 15, no. 1540, 2022. [CrossRef] [Google Scholar] [Publisher link]

[5] Sourav Sarkar, and Manash Chakraborty, "Stability Analysis for Two-Layered Slopes by using the Strength Reduction Method," *International Journal of Geo-Engineering*, vol. 12, no. 24, 2021. [CrossRef] [Google Scholar] [Publisher link]

[6] Henok Marie Shiferaw, "Study on the Influence of Slope Height and Angle on the Factor of Safety and Shape of Failure of Slopes based on Strength Reduction Method of Analysis," *Beni-Suef University Journal of Basic and Applied Sciences*, vol. 10, no. 31, 2021. [CrossRef] [Google Scholar] [Publisher link]

[7] S. M. Seyed-Kolbadi, J. Sadoghi-Yazdi, and M. A. Hariri-Ardebili, "An Improved Strength Reduction-Based Slope Stability Analysis," *Geosciences*, vol. 9, no. 1, 2019. [CrossRef] [Google Scholar] [Publisher link]

[8] Lin Guocai et al., "Study on Rainfall Infiltration, Unsaturated Seepage Process, and Stability Changes of Slopes," *Waterway and Harbor Engineering*, 2019. [Publisher link]

[9] Wei Gangqiang, "*Analysis of Shale Cut Slope Stability under the Effects of Rainfall and Earthquake*," Thesis, Changsha University of Science and Technology, 2020.

[10] Olga Hachay, and Oleg Khachay, "Future of Mining Techniques in Deep Ore Mines without Catastrophic Risks," *SSRG International Journal of Geoinformatics and Geological Science*, vol. 7, no. 1, pp. 23-29, 2020. [CrossRef] [Publisher link]

[11] Olga Hachay, Andrey Khachay, and Oleg Khachay, "Monitoring the Ore Massif State in Deep Rock Shock Mines," *SSRG International Journal of Geoinformatics and Geological Science*, vol. 6, no. 2, pp. 6-13, 2019. [CrossRef] [Publisher link]

[12] Arun Kumar, and M. Sunil Singh, "Back Analysis of Rock Support and Final-Lining Recommendation for Rock Class C1 of a Tunnel," *International Journal of Engineering Trends and Technology*, vol. 71, no. 1, pp. 79-93, 2023. [CrossRef] [Publisher link]

[13] Dharmesh N, and L. Govindaraju, "A Study on Shear Frame Structure by Modal Superposition Method," *International Journal of Engineering Trends and Technology*, vol. 71, no. 2, pp. 457-465, 2023. [CrossRef] [Publisher link]